Molecular Crystals and Liquid Crystals

Publication details, including instructions for authors and subscription information:
http://www.tandfonline.com/loi/gmcl20

Mesomorphic Properties of Diesters with p-Substituted-Arylazomethine Pendant Groups

Sandra A. Hernández [a] & Raúl O. Garay [a]

[a] Instituto de Investigaciones en Química Orgánica, Departamento de Química, Universidad Nacional del Sur, Bahía Blanca, Argentina

Version of record first published: 17 Oct 2011

To cite this article: Sandra A. Hernández & Raúl O. Garay (2006): Mesomorphic Properties of Diesters with p-Substituted-Arylazomethine Pendant Groups, Molecular Crystals and Liquid Crystals, 451:1, 21-32

To link to this article: http://dx.doi.org/10.1080/154214090959984

Mol. Cryst. Liq. Cryst., Vol. 451, pp. 21–32, 2006

ISSN: 1542-1406 print/1563-5287 online
DOI: 10.1080/154214090959984

Taylor & Francis
Taylor & Francis Group

Mesomorphic Properties of Diesters with *p*-Substituted-Arylazomethine Pendant Groups

Sandra A. Hernández
Raúl O. Garay
Instituto de Investigaciones en Química Orgánica, Departamento de Química, Universidad Nacional del Sur, Bahía Blanca, Argentina

The substituent steric and electronic effects on mesophase stability and glass-forming properties of a series of 1,4-bis-(4-n-alkyloxybenzoyloxy)-2-N-(p-Y-aryl) azomethinebenzenes were evaluated. The diesters showed a typical though mild dependence of the monotropic nematic–isotropic transition temperatures on the substituent size that was attributed to the conformational flexibility of the pendant azomethine group. In contrast, the dependence of the entropy change associated with the nematic–isotropic transition showed an atypical behavior ascribed to the extreme reduction of the mesogen axial ratio. The introduction of the bulky arylazomethine group on a lateral position originated significant crystallization supercooling. The appearance of glassy mesophases was detected in some of the diesters; the OEt and CF_3 groups were the more effective substituents to promote the formation of nematic glasses.

Keywords: glassy mesophase; liquid crystal; nematic; substituent effects

INTRODUCTION

Understanding the structure–property relationships has been a major driving force in liquid crystals research. It has been demonstrated that even small structural changes of the mesogens lead to significant variations in their physicochemical and electrooptical properties [1,2]. Among other structural modifications, the effect of lateral substitution

Financial support for this research was provided by Consejo Nacional de Investigaciones Científicas (CONICET), Agencia Nacional para la Promoción Cientifica y Tecnológica (ANPCyT), and Secretaría General de Ciencia y Técnica-Universidad Nacional del Sur (SGCyT).

Address correspondence to R. Garay, INIQO, Departamento de Química, Universidad Nacional del Sur, Alem 1253, 8000 Bahía Blanca, Argentina. E-mail: rgaray@criba.edu.ar

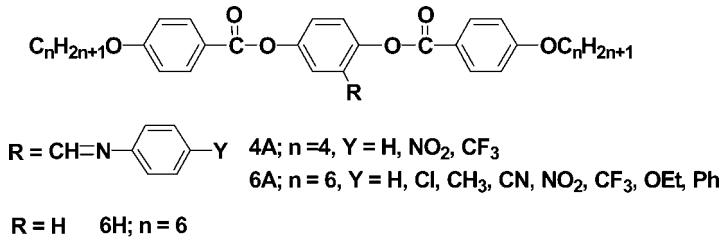

SCHEME 1 Structures and acronyms of the diesters.

on the overall properties of many low-molecular-weight [3–5] and polymeric [6] nematic liquid crystals has been studied in the past decades. Most of the studies refer to systems in which the substituent is directly attached to the mesogenic unit. However, as Gray noted, the relative effect of a lateral substituent on mesophase stability depends not only on the size and polarity of the substituent but also upon the nature of the molecule into which it is introduced [3]. The main purpose of this study is to evaluate the electronic and steric effects on mesophase stability of diesters bearing an *N*-arylazomethine pendant group with a *para*-substituent. Because the substituent groups are not directly attached to the central part of the mesogen but appended instead on a lateral moiety that has conformational flexibility, the consequences of the substitution on the mesomorphic properties are not apparent. The mnemonic used for these compounds is **nA**[Y] where **n** denotes the number of carbon atoms in the alkyl terminal chains, **A** the arylazomethine lateral group and [Y] the substituent in the *para* position in the arylazomethine group.

RESULTS AND DISCUSSION

The transitional properties of the compounds **4A**[Y] and **6A**[Y] are summarized in Table 1 as well as those corresponding to the compound **6H**. Because only the transition temperatures of **6H** are available in the literature, this compound was synthesized to determine its transition enthalpies [7]. The melting points and the liquid crystalline transition temperatures listed are the peak maxima in the DSC traces. Each sample was treated in an identical manner, namely, heated at 10°C min^{-1} into the isotropic phase, then cooled to 30°C at 10°C min^{-1}, held at that temperature, and subsequently reheated into the isotropic phase. Many of the compounds have a tendency to produce several solid modifications and some of them show cold crystallization exotherms or no significant melting endotherms in the second heating cycle. The compounds are monotropic nematogens with the exception of **4A**[NO_2], **6A**[NO_2], and

TABLE 1 Calorimetric Investigation of the **4A** and **6A** Series[a]

	1HC		1CC				
Compound	T_m	ΔH_m	T_m	T_{NI}	ΔH_{NI}	$\Delta S_{NI}/R$	*Tg*
4A[H]	117[b]/128[b]/134	30.0	79–90[c]	(119)	1.61	0.49	
4A[NO_2]	81[b]/95	5.4/34.2	49–64[c]				
4A[CF_3]	89[b]/101	42.7/4.6		(95)	0.88	0.29	2.3
6H	125	32.9	115	215	2.30	0.57	
6A[H]	124	32.8	74–86[c]	(103)	1.62	0.52	
6A[Cl]	123	53.2		(85)	1.25	0.42	
6A[CH_3]	97	42.4		(90)	1.21	0.40	
6A[CN]	127	90.2	73				
6A[NO_2]	115[b]/144	52.5	105–110[d]				
6A[CF_3]	122	48.6		(66)	0.90	0.32	6.0
6A[OEt]	67[b]/87	5.0/30.4		(69)	0.73	0.26	−1.7
6A[Ph]	102	43.4		(59)	0.42	0.15	

[a]T = °C, ΔH = KJ mol^{-1}, ΔS = J mol^{-1}K^{-1}.
[b]T_{CC}.
[c]Broad exotherms with the main peak displaying one or more shoulders.
[d]Detected by optical microscope observations.

6A[CN] for which no mesophase is observed. The nematic phases were assigned from their threaded optical textures.

The dependences upon the substituent van der Waals volumes, V_w, of the transition temperatures as well as the entropy changes associated with the nematic–isotropic transition of the 6A series are shown in Fig. 1. The transitional properties were plotted against V_w, instead of van der Waals radii, r_w, because the former account better for intermolecular distance variations due to substituent changes [8]. The melting points show no regular dependence on V_w. In contrast, the nematic–isotropic transitions as well as the entropy associated with the nematic–isotropic transition regularly decrease with increasing V_w. The dependence of the T_{NI} in **4A** and **6A** series is very typical of that observed in nematogens [3]. Longer terminal chains lead to lower nematic–isotropic transitions. Likewise, the T_{NI} of **4A**[H] and **6A**[H] are significantly lower than those reported for the unsubstituted analogous **4H** (T_{NI} = 245°C) and **6H** (T_{NI} = 211°C) as could be expected from the decrease of the axial ratio of the mesogenic group caused by the azomethine group attachment [7]. Because the $\Delta S_{NI}/R$ remains almost unchanged upon substitution (see entries 4 and 5 in Table 1), the reduction of T_{NI} reflects the decrease in the mesogenic core soft interactions due to the increased biaxiality. Remarkably, even the highly irregular **6A**[Ph] displayed a nematic phase. The moderate

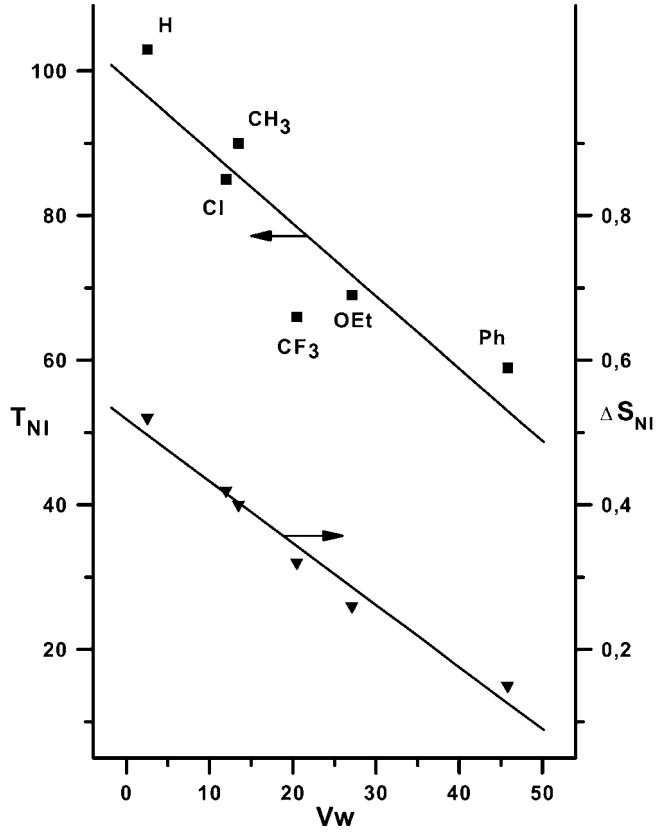

FIGURE 1 The dependence of the nematic–isotropic transition temperatures on the van der Waals volumes of Y for the **6A** series (■) and the dependence of the entropy change associated with the nematic–isotropic transition on the van der Waals volumes of *Y* for the **6A** series (▼).

response of T_{NI} to substituent size can be attributed to the conformational flexibility of the pendant azomethine group that could allow the *p*-aryl substituents to be partially aligned along the longitudinal axis of the mesogenic unit, thus diminishing the effects due to the lateral substituent size. Indeed, computer modeling studies have indicated that the folded conformations (see Fig. 2) are predominant and that their contribution to the conformational equilibria between folded and extended conformations is significant [9]. On the other hand, the similarity between the $\Delta S_{NI}/R$ of **6H** and **6A**[H] as well as its reduction on substitution at the *para* position in the **4A** and **6A** series are surprising results if compared to structurally related compounds for which it is

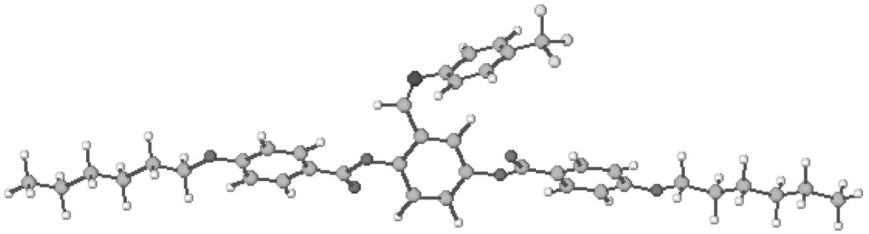

FIGURE 2 PM3 geometry of the folded conformation of **6A**[CF_3].

often found that a lateral substituent in the central aromatic unit of the triad increases $\Delta S_{NI}/R$ [4]. According to Flory, small reductions in the axial ratio would increase $\Delta S_{NI}/R$ until a maximum is reached, and then further reductions would result in a decrease of $\Delta S_{NI}/R$ [10]. In our case, it seems that the large axial ratio dwindling caused by the bulky arylazomethine group leaves the mesogen in the regime where further shortening of the axial ratio results in reductions of $\Delta S_{NI}/R$.

Both **4A**[H] and **6A**[H] showed strong supercooling, but eventually they crystallize in the cooling cycle after revealing the metastable mesophase. However, although the polar nature of the *p*-substituent Y bears no effect on the nematic–isotropic transition, the substitution with strong electronic-acceptor groups led to compounds with a higher tendency to crystallize. Thus, no metastable mesophase was observed for **4A**[NO_2], **6A**[NO_2], and **6A**[CN]. Diesters **4A**[NO_2] and **6A**[CN] distinctly showed only a crystallization exotherm in the cooling cycle with less supercooling than those observed for **4A**[H] and **6A**[H]. However, the DSC trace for **6A**[NO_2] was a flat line, and no transition of either first or second order was recorded in the cooling cycle. However, we were able to repeatedly visualize on the polarizing microscope a crystallization transition at 110°C. The remaining compounds of the **4A** and **6A** series showed the transition to the metastable mesophase but no crystallization exotherm above 30°C in the cooling cycle. It was possible to cycle repeated times between the isotropic and nematic phases on the hot stage of the polarizing microscope without crystallization interference. Yet, some of them, **6A**[Cl], **6A**[CH_3], and **6A**[Ph], crystallized shortly after they reached 20°C in the hot stage of the polarizing microscope. These diesters also displayed cold crystallization exotherms in the DSC traces of the second heating cycle. Finally, diesters **4A**[CF_3], **6A**[CF_3], and **6A**[EtO] showed in the second heating cycle the nematic–isotropic transition and either very small or no cold crystallization exotherms and melting endotherms. Therefore, their thermal behavior was also analyzed in a lower temperature range,

from −40°C to 150°C. At cooling rates of 10°C, the DSC traces showed a second-order transition indicating that all three diesters form glassy nematic phases.

The glass transition temperatures quoted in Table 1 are the inflexion points in the baseline. The DSC traces of the cooling and second heating cycles for the glass-forming diesters **6A**[CF_3] and **6A**[OEt] are shown in Fig. 3, together with the traces corresponding to **6A**[CH_3], which crystallize at room temperature. On heating from the glassy mesophase, **6A**[CF_3] showed significant melting transition and cold crystallization only during and after isotropization, whereas diester **6A**[EtO] showed the glass transition, the nematic–isotropic

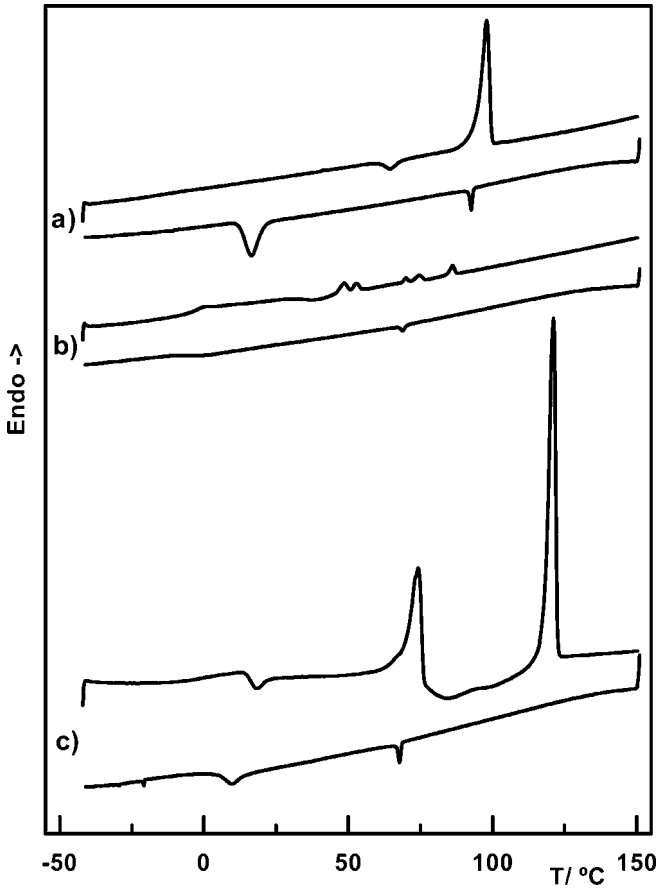

FIGURE 3 DSC traces for the first cooling and second heating cycles of a) **6A**[CH_3], b) **6A**[CF_3], and c) **6A**[OEt].

transition, and very small cold crystallization exotherms and melting endotherms. Analogously, **4A**[CF_3] showed only the glass and the clearing transitions. Therefore, the ethoxy group, with moderate lipophilicity and larger V_W, and the trifluoromethyl group, with very low cohesive energy and low surface free energy (both with moderate polarity but very low polarizability), are the substituents of choice to avoid crystallization. As can be observed in Fig. 3, the substituent groups are forced to lodge in the mesogen polar center even in the folded conformations. Apparently, their lipophilicity and fluorophilicity interfere with the attractive interactions between the polar centers of the mesogens. **6A**[CF_3] and **6A**[CF_3] showed higher glass transition temperatures than **6A**[OEt], though the variation is small. It has been shown that enhanced molecular polarity results in increased glass transition [11]. Though both groups are polar, the electron–donating ethoxy group will oppose the dipole originated by the azomethine group while the electron–withdrawing trifluoromethyl group will reinforce it. Indeed, the molecular dipole moments calculated at the semi-empirical level (PM3) for **6A**[H], **6A**[OEt], and **6A**[CF_3] show the trend 2.11 D, 2.67 D, and 4.15 D, which is similar to the trend reported for liquid crystal derivatives of 4-octyloxy-1-(*p*-Y-arylazomethine)benzene with methoxy and trifluoromethyl groups [12].

In conclusion, we observed a typical though moderate dependence of the monotropic nematic–isotropic transition temperatures on the van der Waals volumes of the substituent that can be attributed to the conformational flexibility of the pendant azomethine group that could allow them to be partially aligned along the mesogen longitudinal axis. In contrast, the dependence of the entropy change associated with the nematic–isotropic transition showed an atypical behavior ascribed to the extreme reduction of the mesogen axial ratio. The introduction on a lateral position of the bulky arylazomethine group originated significant supercooling of the crystallization. The appearance of glassy mesophases was detected in some of the compounds; the OEt and CF_3 groups were more effective in generating nematic glasses.

EXPERIMENTAL

All melting points are uncorrected. Elemental analysis were made in the Universidad de Buenos Aires, INQUIMAE. ^{1}H NMR and ^{13}C NMR spectra were recorded on a Bruker ARX300 spectrometer. Thermal analysis was carried out on a Perkin-Elmer DSC7 instrument equipped with a liquid nitrogen cooling system under a nitrogen flow at scan rates of 10°C/min with samples of about 10 mg. The melt behavior was observed on an optical polarizing microscope (Leitz, Model

Ortolux) equipped with a pair of crossed polarizers and a hot stage (Mettler).

Molecular Modeling

Molecular Modeling of the compounds and molecular dipole moments calculation were carried out at the semi-empirical level using the PM3 MO program [14]. Modeling was assumed to be carried out in the gas phase at 0 K. The minimization operations were performed using the conjugate gradient method and halted by setting the gradient option at 0.01 kcal/mol. The lowest potential energy conformations were found by minimization of the energy function in conjunction with conformation searches around various bonds. Several close energy minima, common to each of the **6A** series members, were found as a result of the high conformational flexibility of the molecules. Though the dipole absolute values of a compound varied for each of the minimum, the trend for each of the minima in the **6A** series members was similar.

Synthesis

The *para*-substituted anilines, 2,5-dihydroxybenzaldehyde and *para*-*n*-hexyloxybenzoyl chloride, were obtained commercially (Aldrich). 4-*n*-Butoxybenzoic acid was prepared according to a method previously described [13], and then the acid was refluxed in thionyl chloride to afford 4-*n*-Butoxybenzoyl chloride. With the exception of the compound with Y = Ph, the synthesis of *N*-(2,5-dihydroxybenzylidene)-*p*-substituted-anilines has been already reported [9].

***N*-(2,5-dihydroxybenzylidene)-*p*-biphenylaniline.** [Y = Ph]. A mixture of 2,5-dihydroxybenzaldehyde (2.5 g, 18.1 mmol) was dissolved in dry methanol (5 ml) under argon, and then a solution of 4′-biphenylaniline (3.06 g, 18.1 mmol) in dry methanol (11 ml) was added at room temperature. After 1 h the reaction mixture was cooled to 5°C, and a yellow precipitate was isolated by filtration. The solid washed with pentane and recrystallized from a mixture of benzene–tetrachloroethane–acetonitrile (3:1:2). Yield: 59%; mp: 186–190°C. ^{1}H NMR (acetone-d_6): 12.52 (s, 1H, OH), 8.86 (s, 1H, HC=N), 8.02 (s, 1H, OH), 7.76 (d, 2H, J_o 8.8 Hz), 7.70 (d, $2H_{o,o'}$, J_o 7.3 Hz), 7.50 (d, 2H, J_o 8.8 Hz), 7.46 (d, $2H_{m,m'}$, J_o 7.3 Hz), 7.38 (t, $1H_p$, J_o 7.3 Hz), 7.07 (d, 1H, J_m 2.9 Hz), 6.98 (dd, 1H, J_o 8.8 Hz and J_m 2.9 Hz), 6.84 (d, 1H, J_o 8.8 Hz). ^{13}C NMR (acetone-d_6): 162.9, 153.1, 149.6, 147.6, 139.4, 138.5, 128.9, 127.6, 127.5, 126.5, 121.4, 121.2, 119.3, 117.3,

116.9. Anal. calcd. for $C_{19}H_{15}NO_2$: C, 78.87; H, 5.23; N, 4.84. Found: C, 79.31: H, 5.28: N, 4.46.

Diesters Synthesis

The Compounds **4A**[Y] and **6A**[Y], as well as **6H**, were prepared by the overnight reaction of the substituted hydroquinones (2.0 mmol) with either *p*-n-hexyloxybenzoyl chloride or 4-*n*-butoxybenzoyl chloride (4.1 mmol) in Cl_2CH_2 (40 ml) in the presence of Et_3N (1.0 ml) at room temperature and purified by several recrystallizations from ethanol. Yields of purified model compounds: 40–70%. The diesters purity was checked by TLC, and then they were fully characterized by ^1H and ^{13}C NMR. The following numbering system to describe the proton and carbons in the range of structurally similar compounds was applied to the ^1H and ^{13}C NMR spectra.

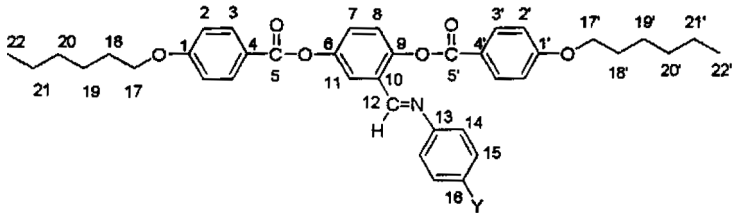

4A[H]. ^1H NMR ($CDCl_3$): 6.97 (d, $4H^{2,2'}$, J_o 8.8), 8.15 (d, $2H^3$, J_o 8.8), 8.14 (d, $2H^{3'}$, J_o 8.8), 7.39 (dd, $1H^7$, J_o 8.8, J_m 2.7), 7.30 (d, $1H^8$, J_o 8.8), 8.08 (d, $1H^{11}$, J_m 2.7), 8.57 (s, $1H^{12}$), 7.34 (d, $2H^{14}$, J_o 8.0), 7.19–7.09 (m, $3H^{15,16}$), 4.05 (t, $2H^{17}$, J 6.6), 4.04 (t, $2H^{17'}$, J 6.6), 1.91–1.77 (m, $4H^{18,18'}$), 1.64–1.46 (m, $4H^{19,19'}$), 0.99 (t, $3H^{20}$, J 6.9), 0.98 (t, $3H^{20'}$, J 6.9). ^{13}C NMR ($CDCl_3$): 163.8 (C^1), 163.6 ($C^{1'}$), 114.5 (C^2), 114.3 ($C^{2'}$), 132.4 (C^3), 132.3 ($C^{3'}$), 121.3 ($C^{4,4'}$), 164.6 ($C^{5,5'}$), 148.4 (C^6), 125.5 (C^7), 121.0 (C^8), 148.8 (C^9), 129.6 (C^{10}), 124.0 (C^{11}), 153.9 (C^{12}), 151.8 (C^{13}), 120.8 (C^{14}), 129.0 (C^{15}), 126.2 (C^{16}), 68.0 ($C^{17,17'}$), 31.0 ($C^{18,18'}$), 19.1 ($C^{19,19'}$), 13.7 ($C^{20,20'}$). Anal. calcd. for $C_{35}H_{35}NO_6$: C, 74.32; H, 6.24; N, 2.48. Found: C, 74.17; H, 6.28; N, 2.27.

4A[NO2]. ^1H NMR ($CDCl_3$): 6.97 (d, $4H^{2,2'}$, J_o 8.8), 8.16 (d, $4H^{3,3'}$, J_o 8.8), 7.45 (dd, $1H^7$, J_o 8.8, J_m 2.7), 7.33 (d, $1H^8$, J_o 8.8), 8.08 (d, $1H^{11}$, J_m 2.7), 8.52 (s, $1H^{12}$), 7.13 (d, $2H^{14}$, J_o 8.0), 8.19 (d, $2H^{15,16}$, J_o 8.8), 4.06 (t, $2H^{17}$, J 6.6), 4.05 (t, $2H^{17'}$, J 6.6), 1.88–1.74 (m, $4H^{18,18'}$), 1.61–1.42 (m, $4H^{19,19'}$), 0.99 (t, $6H^{20,20'}$, J 6.9). ^{13}C NMR ($CDCl_3$): 164.9, 163.7, 114.5, 114.4, 132.4, 132.3, 120.8, 164.6, 148.8, 125.6, 121.4, 148.9, 128.8, 124.2, 156.5, 157.5, 121.1, 129.1, 145.6 (C^{16}), 68.0, 31.0, 19.1, 13.7. Anal. calcd. for $C_{35}H_{34}N_2O_8$: C, 68.84; H, 5.61; N, 4.59. Found: C, 68.68; H, 5.55; N, 4.35.

4A[CF_3]. ^{1}H NMR ($CDCl_3$): 6.98 (d, 4H$^{2,2'}$, J_o 8.8), 8.15 (d, 4H$^{3,3'}$, J_o 8.8), 7.44 (dd, 1H^7, J_o 8.8, J_m 2.7), 7.31 (d, 1H^8, J_o 8.8), 8.08 (d, 1H^{11}, J_m 2.7), 8.52 (s, 1H^{12}), 7.57 (d, 2H^{14}, J_o 8.0), 7.14 (d, 2H^{15,16}, J_o 8.8), 4.06 (t, 2H$^{17,17'}$, J 6.6), 1.91–1.77 (m, 4H$^{18,18'}$), 1.64–1.45 (m, 4H$^{19,19'}$), 0.99 (t, 6H$^{20,20'}$, J 6.9). ^{13}C NMR ($CDCl_3$): 164.0, 163.7, 114.4, 114.3, 132.3, 132.2, 121.2 (C^4), 121.1 (C$^{4'}$), 164.6, 148.6, 126.1, 121.2, 148.8, 129.1, 124.1, 155.8, 154.9, 120.9 (q, C^{14}, $^4J_{14}$ 1.0), 126.2 (q, C^{15}, $^3J_{15}$ 4.0), 127.9 (q, C^{16}, $^2J_{16}$ 32.2), 68.0, 31.0, 19.1, 13.7, 123.8 (q, CF_3, $^1J_{CF3}$ 273.0). Anal. calcd. for $C_{36}H_{34}F_3NO_6$: C, 68.24; H, 5.41; N, 2.21. Found: C, 68.07; H, 5.35; N, 2.17.

6H. ^{1}H NMR ($CDCl_3$): 6.96 (d, 4H$^{2,2'}$, J_o 8.9), 8.13 (d, 4H$^{3,3'}J_o$ 8.9), 7.25 (s, 4H^{7,8}), 4.03 (t, 4H$^{17,17'}J$ 6.6), 1.86–1.75 (m, 4H$^{18,18'}$), 1.53–1.26 (m, 12H$^{19,19',20,20',21,21'}$), 0.91 (t, 6H$^{22,22'}J$ 7.0).^{13}C NMR ($CDCl_3$): 163.6, 114.3, 132.3, 121.4, 164.8, 148.4, 122.6, 68.3, 31.5, 25.6, 29.0, 22.6, 14.0.

6A[H]. ^{1}H NMR ($CDCl_3$): 6.98 (d, 4H$^{2,2'}$, J_o 8.8), 8.16 (d, 2H^3, J_o 8.8), 8.15 (d, 2H$^{3'}$, J_o 8.8), 7.40 (dd, 1H^7, J_o 8.8, J_m 2.7), 7.31 (d, 1H^8, J_o 8.8), 8.09 (d, 1H^{11}, J_m 2.7), 8.58 (s, 1H^{12}), 7.35 (d, 2H^{14}, J_o 8.0), 7.20–7.10 (m, 3H^{15,16}), 4.05 (t, 2H^{17}, J 6.6), 4.04 (t, 2H$^{17'}$, J 6.6), 1.89–1.76 (m, 4H$^{18,18'}$), 1.53–1.34 (m, 12H$^{19,19',20,20',21,21'}$), 0.92 (t, 3H^{22}, J 6.9), 0.91 (t, 3H$^{22'}$, J 6.9). ^{13}C NMR ($CDCl_3$): 163.9 (C^1), 163.7 (C$^{1'}$), 114.5 (C^2), 114.4 (C$^{2'}$), 132.4 (C^3), 132.3 (C$^{3'}$), 121.1(C^4), 120.8 (C$^{4'}$), 164.6 (C$^{5,5'}$), 148.5 (C^6), 125.5 (C^7), 121.1 (C^8), 148.9 (C^9), 129.7 (C^{10}), 124.0 (C^{11}), 154.0 (C^{12}), 151.8 (C^{13}), 120.8 (C^{14}), 129.1 (C^{15}), 126.2 (C^{16}), 68.4/68.3 (C$^{17,17'}$), 31.5 (C$^{18,18'}$), 25.6 (C$^{19,19'}$), 29.1/29.0 (C$^{20,20'}$), 22.5 (C$^{21,21'}$), 13.9 (C$^{22,22'}$).

6A[Cl]. ^{1}H NMR ($CDCl_3$): 6.99 (d, 2H^2, J_o 8.8), 6.98 (d, 2H$^{2'}$, J_o 8.8), 8.16 (d, 2H^3, J_o 8.8), 8.15 (d, 2H$^{3'}$, J_o 8.8), 7.41 (dd, 1H^7, J_o 8.8, J_m 2.7), 7.31 (d, 1H^8, J_o 8.8), 8.07 (d, 1H^{11}, J_m 2.7), 8.54 (s, 1H^{12}), 7.28 (d, 2H^{14}, J_o 8.8), 7.03 (m, 2H^{15}, J_o 8.8), 4.05 (t, 4H$^{17,17'}$, J 6.6), 1.90–1.76 (m, 4H$^{18,18'}$), 1.54–1.31 (m, 12H$^{19,19',20,20',21,21'}$), 0.92 (t, 6H$^{22,22'}$, J 6.9). ^{13}C NMR ($CDCl_3$): 163.9, 163.7, 114.5, 114.3, 132.4, 132.3, 121.2, 121.1, 164.6, 148.5, 125.7, 121.1, 148.8, 129.3, 124.0, 154.2, 150.2, 122.1, 129.1, 131.8 (C^{16}), 68.4/68.3, 31.5, 25.6, 29.0/28.9, 22.5, 13.9.

6A[CH_3]. ^{1}H NMR ($CDCl_3$): 7.00 (d, 2H^2, J_o 8.8), 6.98 (d, 2H$^{2'}$, J_o 8.8), 8.15 (d, 2H^3, J_o 8.8), 8.14 (d, 2H$^{3'}$, J_o 8.8), 7.38 (dd, 1H^7, J_o 8.8, J_m 2.7), 7.30 (d, 1H^8, J_o 8.8), 8.08 (d, 1H^{11}, J_m 2.7), 8.58 (s, 1H^{12}), 6.96 (d, 2H^{14}, J_o 8.0), 7.12 (m, 2H^{15}, J_o 8.0), 4.05 (t, 4H$^{17,17'}$, J6.6), 1.89–1.76 (m, 4H$^{18,18'}$), 1.54–1.32 (m, 12H$^{19,19',20,20',21,21'}$), 0.91 (t, 6H$^{22,22'}$, J 6.9), 2.32 (s, 3H, CH_3). ^{13}C NMR ($CDCl_3$): 163.8, 163.6, 114.5, 114.3, 132.4, 132.3, 121.1, 120.8, 164.6, 148.3, 125.3, 121.0, 148.9, 129.7, 123.9, 153.1, 149.2, 120.7, 129.6, 136.1 (C^{16}), 68.3/∼68.3, 31.5, 25.6, 29.0, 22.5, 13.9, 20.9 (CH_3).

6A[CN]. ^{1}H NMR ($CDCl_3$): 6.97 (d, 4H^{2}, J_o 8.8), 8.14 (d, 2H^{3}, J_o 8.8), 8.13 (d, 2H$^{3'}$, J_o 8.8), 7.43 (dd, 1H^{7}, J_o 8.8, J_m 2.7), 7.30 (d, 1H^{8}, J_o 8.8), 8.06 (d, 1H^{11}, J_m 2.7), 8.49 (s, 1H^{12}), 7.10 (d, 2H^{14}, J_o 8.0), 7.60 (m, 2H^{15}, J_o 8.0), 4.05 (t, 4H$^{17,17'}$, J 6.6), 1.89–1.76 (m, 4H$^{18,18'}$), 1.53–1.31 (m, 12H$^{19,19',20,20',21,21'}$), 0.91 (t, 6H$^{22,22'}$, J 6.9). ^{13}C NMR ($CDCl_3$): 163.9, 163.7, 114.3, 114.2, 132.3, 132.2, 121.0, 120.9, 164.6, 148.7, 125.3, 121.3, 148.9, 128.8, 124.2, 156.2, 155.6, 121.4, 133.3, 100.8 (C^{16}), 68.3/∼68.3, 31.4, 25.5, 28.9, 22.5, 13.9, 120.3 (CN).

6A[NO2]. ^{1}H NMR ($CDCl_3$): 6.98 (d, 4H$^{2;}$ J_o 8.8), 8.14 (d, 4H$^{3,3'}$, J_o 8.8), 7.44 (dd, 1H^{7}, J_o 8.8, J_m 2.7), 7.33 (d, 1H^{8}, J_o 8.8), 8.09 (d, 1H^{11}, J_m 2.7), 8.51 (s, 1H^{12}), 7.12 (d, 2H^{14}, J_o 8.0), 8.18 (m, 2H^{15}, J_o 8.0), 4.05 (t, 4H^{17}, J 6.6), 4.04 (t, 4H$^{17'}$, J 6.6), 1.89–1.78 (m, 4H$^{18,18'}$), 1.52–1.32 (m, 12H$^{19,19',20,20',21,21'}$), 0.92 (t, 6H^{22}, J 6.9), 0.91 (t, 6H$^{22'}$, J 6.9). ^{13}C NMR ($CDCl_3$): 164.0, 163.7, 114.6, 114.4, 132.4, 132.3, 121.0, 121.0, 164.6, 148.8, 125.6, 121.4, 148.9, 128.8, 124.2, 156.5, 157.5, 121.1, 129.1, 145.6, 68.4/68.3, 31.4, 25.6, 29.0/28.9, 22.5, 13.9.

6A[CF_3]. ^{1}H NMR ($CDCl_3$): 6.98 (d, 4H$^{2;}$ J_o 8.8), 8.15 (d, 4H$^{3,3'}$, J_o 8.8), 7.43 (dd, 1H^{7}, J_o 8.8, J_m 2.7), 7.32 (d, 1H^{8}, J_o 8.8), 8.08 (d, 1H^{11}, J_m 2.7), 8.53 (s, 1H^{12}), 7.57 (d, 2H^{14}, J_o 8.0), 7.13 (m, 2H^{15}, J_o 8.0), 4.05 (t, 4H^{17}, J 6.6), 4.04 (t, 4H$^{17'}$, J 6.6), 1.89–1.76 (m, 4H$^{18,18'}$), 1.53–1.34 (m, 12H$^{19,19',20,20',21,21'}$), 0.92 (t, 6H^{22}, J 6.9), 0.91 (t, 6H$^{22'}$, J 6.9). ^{13}C NMR ($CDCl_3$): 164.0, 163.7, 114.6, 114.4, 132.4, 132.3, 120.9, 120.6, 164.6, 148.7, 126.2, 121.3, 148.9, 129.1, 124.2, 155.8, 154.9, 120.9 (q, C^{14}, $^{4}J_{14,F}$ 1.0), 126.3 (q, C^{15}, $^{3}J_{15,F}$ 4.0), 127.3 (q, C^{16}, $^{2}J_{16,F}$ 32.7), 68.4/68.3, 31.5/31.4, 25.6, 29.0/∼29.0, 22.5, 13.9, 123.8 (q, CF_3, $^{1}J_{CF3}$ 272.0).

6A[OEt]. ^{1}H NMR ($CDCl_3$): 6.98 (d, 2H^{2}; J_o 8.8), 6.97 (d, 2H$^{2'}$; J_o 8.8), 8.16 (d, 2H^{3}, J_o 8.8), 8.14 (d, 2H$^{3'}$, J_o 8.8), 7.36 (dd, 1H^{7}, J_o 8.8, J_m 2.7), 7.28 (d, 1H^{8}, J_o 8.8), 8.06 (d, 1H^{11}, J_m 2.7), 8.58 (s, 1H^{12}), 7.10 (d, 2H^{14}, J_o 8.8), 6.82 (m, 2H^{15}, J_o 8.8), 4.05 (t, 4H$^{17,17'}$, J 6.6), 1.89–1.76 (m, 4H$^{18,18'}$), 1.53–1.34 (m, 12H$^{19,19',20,20',21,21'}$), 0.91 (t, 6H$^{22,22'}$, J 6.9), 4.00 (c, CH_2, J 6.9), 1.37 (t, CH_3, J 6.9). ^{13}C NMR ($CDCl_3$): 163.8, 163.6, 114.5, 114.3, 132.3, 132.2, 121.3, 121.3, 164.6, 148.2, 125.0, 120.9, 148.8, 129.9, 123.9, 151.5, 144.4, 122.2, 114.9, 157.9, 68.3/∼68.3, 31.5/31.5, 25.6, 29.0/∼29.0, 22.5, 13.9, 63.6 (CH_2), 14.9 (CH_3).

6A[Ph]. ^{1}H NMR ($CDCl_3$): 6.98 (d, 2H^{2}, J_o 8.8), 6.97 (d, 2H$^{2'}$, J_o 8.8), 8.16 (d, 2H^{3}, J_o 8.8), 8.15 (d, 2H$^{3'}$, J_o 8.8), 7.41 (dd, 1H^{7}, J_o 8.8, J_m 2.7), 7.32 (d, 1H^{8}, J_o 8.8), 8.10 (d, 1H^{11}, J_m 2.7), 8.64 (s, 1H^{12}), 7.56 (d, 2H^{14}, J_o 8.8), 7.18 (m, 2H^{15}, J_o 8.8), 4.05 (t, 2H^{17}, J 6.6), 4.04 (t, 2H$^{17'}$, J6.6), 1.88–1.76 (m, 4H$^{18,18'}$), 1.54–1.32 (m, 12H$^{19,19',20,20',21,21'}$), 0.92 (t, 3H^{22}, J 6.9), 0.91 (t, 3H$^{22'}$, J 6.9), 7.56 (d, J$_o$ 8.8, 2H *o, o′*), 7.44–7.26 (m, 3H *m, m′, p*). ^{13}C NMR ($CDCl_3$): 163.8, 163.6, 114.5, 114.3, 132.3,

132.2, 121.0, 120.7, 164.6, 148.7, 125.5, 121.2, 148.8, 129.6, 124.0, 153.7, 150.8, 121.3, 126.8, 139.1, 68.3/∼68.3, 31.4/∼31.4, 25.5, 29.0/∼29,0, 22.5, 13.9, 140.4 (Ph, *ipso*), 126.8 (Ph, *o, o′)*, 128,7 (Ph, *m, m′)*, 127.7 (Ph, *p*). Anal. calcd. for $C_{45}H_{47}NO_6$: C, 77.45; H, 6.79; N, 2.01. Found: C, 77.38; H, 6.80; N, 1.90.

REFERENCES

[1] Gray, G. W. (Ed.). (1987). *Thermotropic liquid crystals; critical reports in applied chemistry*, Wiley: Great Britain, Chichester, New York, Vol. 22.
[2] Hall, A. W. *et al*. (1997). In: *Handbook of Liquid Crystal Research*, Collings, P. J. & Patel, J. S. (Eds.), Oxford University Press: New York, Chapter 2, 27.
[3] Gray, G. W. (1966). *Mol. Cryst. Liq. Cryst.*, *1*, 333.
[4] Dewar, M. J. S. & Griffin, A. C. (1975). *J. Am. Chem. Soc.*, *97*, 6662.
[5] Bezborodov, V. S. & Petrov, V. F. (1997). *Liq. Cryst.*, *23*, 771.
[6] Lenz, R. W. (1985). *Pure Appl. Chem.*, *57*, 1537.
[7] Weissflog, W. & Demus, D. (1984). *Crystal Res. Technol.*, *19*, 55.
[8] Osman, M. A. (1985). *Mol. Cryst. Liq. Cryst.*, *128*, 45.
[9] Hernandez, S. A., Garay, R. O., Zhou, Q.-F., & Yang, Y.-H. (2000). *Polymer Bulletin*, *45*, 31.
[10] Flory, P. J. & Ronca, G. (1979). *Mol. Cryst. Liq. Cryst.*, *54*, 311.
[11] Wedler, W., Demus, D., Zaschke, H., Mohr, K., Schaefer, W., & Weissflog, W. (1991). *J. Mater. Chem.*, *1*, 347.
[12] Miyajima, S., Nakazato, A., Sakoda, N., & Chiba, T. (1995). *Liq. Cryst.*, *18*, 651.
[13] Gray, G. W. & Jones, B. (1953). *J. Chem. Soc.*, 4179.